

Past, present and future of a meandering river in the Bolivian Amazon basin

Kattia Rubi Arnez Ferrel¹  | Jonathan Mark Nelson²  | Yasuyuki Shimizu¹  | Tomoko Kyuka¹ 

¹Graduate School of Engineering, Hokkaido University, Sapporo, Japan

²U.S. Geological Survey, Golden, Colorado, USA

Correspondence

Kattia Rubi Arnez Ferrel, Graduate School of Engineering, Hokkaido University, Sapporo 060-0808, Japan.

Email: rubikraf@gmail.com

Funding information

Nitobe School Project

Abstract

Field observations on small rivers of the Amazon basin are less common due to their remote location and difficult accessibility. Here we show, through remote sensing analysis and field works, the planform evolution and riverbed topography of a small river located in the upper foreland Amazon basin, the Ichilo River. By tracking planform changes over 30 years, we identified the factors that control meander migration rates in the Ichilo River: cutoffs, climate and human interventions. The data suggest that neck cutoffs are the main controls in the Ichilo River, with an annual density of 0.022 cutoffs/km. In addition, climate controls have been identified in the form of high-precipitation events that may have promoted cutoffs, an increase in meander migration rate and channel widening. The width distribution of the Ichilo River is well represented by general extreme value and inverse Gaussian distributions. The spatio-temporal variability of meandering migration rates in the Ichilo River is analysed in two locations where neck cutoffs are expected. Analysing the distance across the neck in these two points, we predict the occurrence of a new cutoff. The combined methodology of bathymetric surveys and structure from motion photogrammetry shows us the Ichilo riverbed topography and banks at high resolution, where two scour holes were identified. Finally, we discuss the impact of planform changes of the Ichilo River on communities that are established along its riverbanks.

KEY WORDS

bathymetric surveys, Bolivian Amazon basin, Ichilo River, meanders, remote sensing, UAV

1 | INTRODUCTION

The Amazon basin exhibits a constantly changing landscape modified by the rivers that flow through its floodplains. There, we can find many of the fastest meandering rivers in the world, where cutoffs, oxbow lakes and meandering scars are evidence of the evolution that these rivers have experienced over time.

Numerous riverine communities have been established along meandering rivers of the Amazon basin. These communities depend on the abundant natural resources available, where their main economic activities include fishery, agriculture and navigation. Although riverine communities show a strong dependency on river activity (Lombardo, 2016), the morphodynamics of meandering rivers are also

affected by human activity, even changing their planform shape and bend meander migration rates (Schwenk & Foufoula-Georgiou, 2016). However, it is not only human-induced activities that affect the planform configuration of this meandering system, but also natural perturbations. A meander neck cutoff is a natural perturbation that occurs when the river intersects itself (Schwenk & Foufoula-Georgiou, 2016; Schwenk et al., 2015), modifying its current planform configuration. Bend development and sinuosity growth are limited by the occurrence of cutoffs (Van Dijk, 2013). Previous studies have demonstrated that neck cutoffs heavily influence the development of meandering rivers in terms of planform shape, hydraulics and sedimentology, both in the short and long term (Camporeale et al., 2008; Li et al., 2020; Schwenk & Foufoula-Georgiou, 2016).

This is an open access article under the terms of the Creative Commons Attribution-NonCommercial-NoDerivs License, which permits use and distribution in any medium, provided the original work is properly cited, the use is non-commercial and no modifications or adaptations are made.

© 2020 The Authors. *Earth Surface Processes and Landforms* published by John Wiley & Sons Ltd. This article has been contributed to by US Government employees and their work is in the public domain in the USA.

Different approaches have been used to understand, quantify and model meandering rivers in the Amazon basin. Researchers have exploited the potential of remote sensing (Gomes et al., 2018; Lombardo, 2016; Schwenk & Foufoula-Georgiou, 2016; Schwenk et al., 2017), field works and numerical models to study the planform morphodynamics of these rivers. Each methodology, with its advantages and limitations, highlights the importance of integrating different approaches in a complementary way to investigate meandering rivers whenever possible (Van Dijk, 2013).

Most of the research carried out in the Amazon basin is concentrated on the main tributaries of the Amazon River (Lombardo, 2016), while the number of studies in small rivers is limited, especially in the upper foreland Amazon basin, due to their remote location and difficult accessibility. However, a large part of the Amazon network is composed of 'small rivers' (Strahler stream order less than 7) (Lombardo, 2016). Meandering rivers in the upper Amazon basin that are located close to the Andes range have interesting characteristics, such as hydrological cycles with numerous peaks around the year (even in the low season), short inundation periods and high sediment transport, regardless of their low discharge when compared to rivers of the central and low Amazon basin (Lombardo, 2016; Rejas, 2018). There is a need to understand the morphodynamics of rivers in the upper foreland Amazon basin.

This paper explores the planform morphodynamics and bed topography of the Ichilo River, a small meandering river in the upper part of the Bolivian Amazon basin, in order to identify controls on meander migration and planform evolution, such as neck cutoffs,

climate and anthropogenic interventions. We discuss bank erosion and bank accretion processes, the spatial variation of the meander migration rates and future planform evolution of the Ichilo River. Also, we discuss how changes in the river have and will impact the riverine communities established on the Ichilo River.

Our study is divided into two parts. In the first part, the temporal and spatial evolution of the Ichilo River is studied using remote sensing analysis for a period of 30 years in order to understand the planform morphodynamics of the river.

In the second part, we present the results of two field campaigns that were performed in order to collect bathymetric data using a multibeam echosounder (MBES) and investigate bank and bed erosion processes using structure from motion (SfM) photogrammetry. Finally, the results are analysed together, and we discuss the planform changes during the last 30 years and the future planform development of the Ichilo River, with emphasis on the impact it may cause on the inhabitants of its riverbanks.

2 | AREA OF STUDY

The Ichilo River belongs to the upper part of the Amazon basin in Bolivia. It serves as a natural border between the departments of Santa Cruz and Cochabamba (Figure 1). The Ichilo River meanders from south to north from the Andes range to the Bolivian savannah forest. The river reach of the Ichilo presents a single-thread meandering configuration that starts almost immediately after

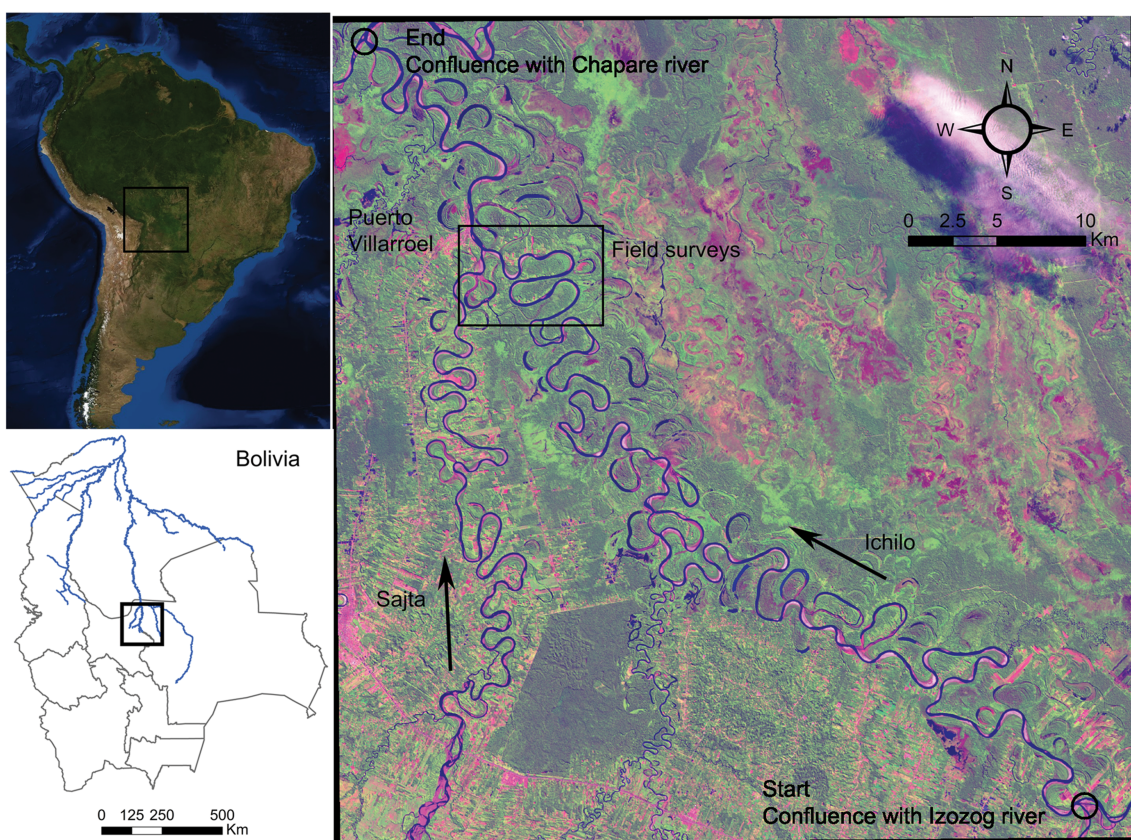


FIGURE 1 Location of the Ichilo River and its tributary in Bolivia. The circles mark the beginning and end of the analysed reach for the satellite imagery analysis and the location of the city of Puerto Villarreal in the department of Cochabamba. The area marked in a rectangle shows where field works were performed [Colour figure can be viewed at wileyonlinelibrary.com]

leaving the Andes mountains, where the alluvial plain starts, and the steep of the terrain decreases noticeably (Peters, 1998). The Ichilo River has many tributaries, such as the Vibora, Izozog, Isarzama and Sajta rivers, among others. The Sajta is an important tributary because it connects with the Ichilo near the city of Puerto Villarroel. The Ichilo River and its tributaries end up in the Mamorecillo River and continue flowing, until they become the Mamoré River. The Ichilo River is the Andean tributary of the Mamore River, which later joins the Madeira River and then reaches the Amazon.

The Ichilo River is characterized as being an active migrating river with high sinuosity. Cutoffs, oxbow lakes, paleochannels and meandering scars from old paths of the Ichilo River remain as testimony of this behaviour.

Recently, the study of Lombardo (2016) has reported annual average migration rates of 0.034 channel widths/year, and an average annual width of 134.2 ± 19.35 m for the Ichilo River. The water levels

in the Ichilo River show high variability, where peaks are observed even during the dry season (June to October), when water levels are the lowest (Figures 2a-c).

Water level data were analysed and the statistics of the annual water levels are presented in Figure 2b. The dataset consists of 31 years of daily water levels, ranging from 1988 to 2019. Figure 2b presents three sets of data: (1) the annual maximum water level (blue asterisks); (2) the annual minimum water level (red dots); and (3) the mean annual water level (yellow squares). The data show that water levels each year decreased below the 2 m level and reached values higher than 6 m. The maximum water levels exceeded the flooding level (7.83 m) affecting the city of Puerto Villarroel with inundations in the years 2019–2016, 2014, 2013, 2010–2007, 2003, 1995 and 1992 (Figure 3). The water level data are collected at the port by local institutions (Servicio de Mejoramiento de la Navegación Amazónica-SEMEA); data are available upon request at <https://www.semena.gob.bo/>.

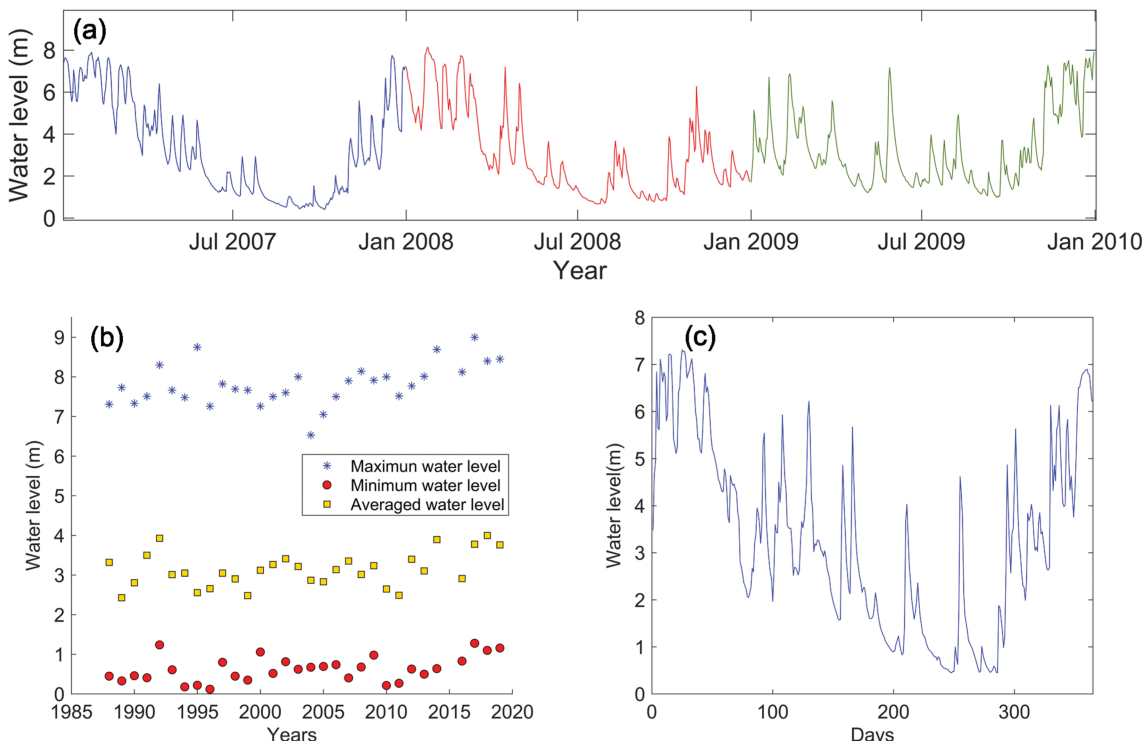


FIGURE 2 (a) Water level measurements from January 2007 to January 2010 for the Ichilo River; (b) annual maximum, averaged and minimum values of water levels observed from 1988 to 2019; (c) daily water level variation on year 1988 [Colour figure can be viewed at wileyonlinelibrary.com]



FIGURE 3 (a) Flooding in Puerto Villarroel (El clíper) in 2018.

Source: Local newspaper los Tiempos. (b) The same point located during the normal stage in February 2019 [Colour figure can be viewed at wileyonlinelibrary.com]

From 1988 to 2018, a total of 10 cutoffs were observed in a length of around 150 km of the Ichilo River, which indicates a density of 0.022 cutoffs/km per year. One of these cutoffs corresponds to a human-induced cutoff designed by Peters (1998) in order to avoid a natural cutoff (Figure 4a), expected to occur during the year 1996–1997. The objective of this human-induced cutoff was to protect a port (Puerto Villarroel) that had been constructed in the banks of the Ichilo River and remains there today (Figure 4b). In terms of area, this cutoff is the largest observed during the studied period.

3 | METHODOLOGY

Here, a combination of remote sensing analysis and field measurements was used to study the active meandering behaviour of the Ichilo River. The remote sensing analysis corresponded to a spatial and temporal analysis for a period of 30 years (1988–2018). Field data were acquired during two field campaigns performed at the Ichilo River during the rainy season in February and May 2019, respectively. During the first campaign, orthophotos were collected using unmanned aerial vehicles (UAVs), and a pocket erodometer test (PET) was performed on the banks of the Ichilo River to check the erodibility of the bank material. The second campaign (May) had the objective of performing a bathymetric survey using a MBES complemented with SfM.

3.1 | History of Ichilo River from satellite imagery

Satellite imagery of the area of study of the Ichilo River was downloaded from Landsat 5 (L5) and Landsat 8 (L8) using the Google Earth Engine (GEE) (Gorelick et al., 2017). The analysis started upstream in the confluence of the Ichilo River with the Izozog River and continued 150 km along the Ichilo River until the confluence with the Chapare River (Figure 1).

The analysis period was from 1988 to 2018, a period of 30 years, and we tried to obtain imagery at an annual time scale. However, in all years, most of the imagery was partially or totally covered by cloud, especially during the rainy season (November to May). The classification and the creation of channel masks was performed similarly to in Schwenk et al. (2017).

3.1.1 | Classification of satellite imagery

Each year the satellite imagery was analysed, searching for cloud-free images for the area of study for the period of low flow (from June to October), except in 2008, when we used an image from the month of November. Only cloud-free images were considered in the analysis, and the dataset used for the analysis is shown in Table 1.

The main objective of the imagery analysis was to obtain a well-defined full channel mask of the river for each year. Each image was classified using a support vector machine (SVM) classification model using the GGE. The classification of the imagery followed three steps: training data, classifying and assessment. The first step consisted of collecting training data of the known pixel

TABLE 1 Imagery considered in the analysis

1988	LANDSAT/LT05/C01/T1/LT05_232072_19880619
1991	LANDSAT/LT05/C01/T1/LT05_232072_19910612
1993	LANDSAT/LT05/C01/T1/LT05_232072_19930804
1994	LANDSAT/LT05/C01/T1/LT05_232072_19940807
1995	LANDSAT/LT05/C01/T1/LT05_232072_19950623
1996	LANDSAT/LT05/C01/T1/LT05_232072_19960609
1998	LANDSAT/LT05/C01/T1/LT05_232072_19980717
1999	LANDSAT/LT05/C01/T1/LT05_232072_19990602
2001	LANDSAT/LT05/C01/T1/LT05_232072_20010810
2003	LANDSAT/LT05/C01/T1/LT05_232072_20030731
2004	LANDSAT/LT05/C01/T1/LT05_232072_20040802
2005	LANDSAT/LT05/C01/T1/LT05_232072_20050720
2006	LANDSAT/LT05/C01/T1/LT05_232072_20060723
2008	LANDSAT/LT05/C01/T1/LT05_232072_20081219
2009	LANDSAT/LT05/C01/T1/LT05_232072_20090901
2010	LANDSAT/LT05/C01/T1/LT05_232072_20101006
2011	LANDSAT/LT05/C01/T1/LT05_232072_20110806
2013	LANDSAT/LC08/C01/T1_RT/LC08_232072_20130726
2014	LANDSAT/LC08/C01/T1_RT/LC08_232072_20141017
2015	LANDSAT/LC08/C01/T1_RT/LC08_232072_20151020
2016	LANDSAT/LC08/C01/T1_RT/LC08_232072_20160702
2017	LANDSAT/LC08/C01/T1_RT/LC08_232072_20170822
2018	LANDSAT/LC08/C01/T1_RT/LC08_232072_20180622

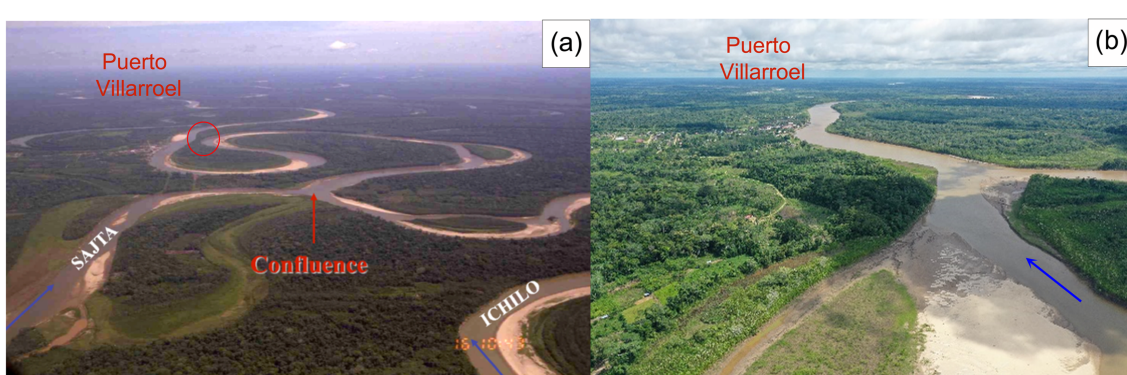


FIGURE 4 Comparison of the evolution of Ichilo River before and after human-induced cutoff. (a) Picture taken before the occurrence of the human-induced cutoff; red circle indicates the location where the natural cutoff was expected.

Source: Peters (2009). (b) Picture taken with a drone in February 2019, 22 years after the human-induced cutoff was executed [Colour figure can be viewed at wileyonlinelibrary.com]

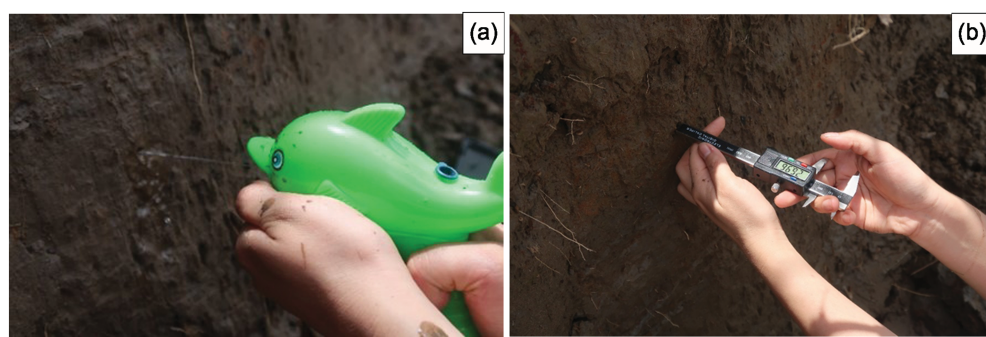


FIGURE 5 Pocket erodometer test in Ichilo River: (a) mini jet pulse device used in the experiment; (b) measurement of the depth using a digital caliper [Colour figure can be viewed at wileyonlinelibrary.com]

classes in each imagery: water, vegetation and sediment. Then, the classification was performed using a SVM classification model. After the classification, a cleaning process was performed manually following the methodology of Schwenk et al. (2017). As a result of the classification, we obtained binary images with a defined channel, and the information was used as input for the analysis of the planform metrics.

3.1.2 | Planform analysis

The analysis of the planforms was performed using the RivMAP (River Morphodynamics from Analysis of Planforms) toolbox (Schwenk et al., 2017). RivMAP consists of a combination of MATLAB codes based on the image-processing morphological operations offered by MATLAB (Schwenk et al., 2017). This toolbox was developed to calculate the metrics of meandering rivers from channel masks as input. The following information was quantified with the toolbox: centrelines, banklines, river widths, migrated areas, cutoffs, erosion and accretion rates (see Schwenk et al., 2017 for more information on the RivMAP toolbox).

In addition, the extracted river widths along the Ichilo River were analysed in order to assess their spatiotemporal distribution. In general, a general extreme value (GEV) distribution provides the best data fit for width sequences in meandering rivers (Lopez Dubon & Lanzoni, 2019). For each year, different probability distribution functions (PDFs) were tested to fit the annual histograms of the dimensionless widths and the most appropriate function was selected using a Bayesian information criterion (BIC), as suggested by Lopez Dubon and Lanzoni (2019).

3.2 | Field measurements

As mentioned before, two field surveys were performed during February and May 2019 to acquire data. During the first field campaign (February 2019) we used a UAV to capture orthophotos along one bend of the Ichilo River where a cutoff is expected (#F1). The objective of this campaign was to identify areas of bank erosion by taking orthophotos with the UAV and assess the location in order to perform a second, more complete field campaign. Also, field measurements of the erodibility of the bank in the Ichilo River were made using a PET (Briaud et al., 2012). This method provides an idea of the soil erodibility using small, inexpensive apparatus that was easy to carry to the location.

TABLE 2 Measured depths with the PET and erosion category of the soil in the riverbank of the Ichilo River

	A	B	C	D	Averaged
PET erosion depth (mm)	26	25	5.5	18.4	18.7
Erosion category	II	II	III	II	II

The methodology consisted of shooting a horizontal jet of water into the vertical face of the bank using a mini jet pulse device (a water gun pistol, Figure 5a).

Pulses of water were squeezed at an interval of 1 s, with a repetition of 20 times. The depth of the hole was measured using a digital calliper (Figure 5b).

The procedure was repeated four times along the bank, and then the measured depth was introduced in the PET table (from Briaud et al., 2012) to determine the erodibility category of the soil among five categories: very high erodibility (I); high erodibility (II); medium erodibility (III); low erodibility (IV); and very low erodibility (V). The results of the test in the Ichilo River are shown in Table 2. The PET erosion category was II, showing a soil of high erodibility (15–75 mm). The detailed methodology of the PET is described in Briaud et al. (2012).

During the second field campaign, topographic data from the banks were obtained by applying SfM photogrammetry. We surveyed the banks using a DJI Phantom 4 Pro and a DJI Mavic Pro was used for taking pictures. Details of the equipment, survey design and execution, and other details, are shown below as suggested in James et al. (2019). The Phantom 4 Pro is equipped with a FC6310S camera that uses a 1-inch CMOS sensor at 20 megapixels with an aperture range from F2.8 to F11 and a 24 mm equivalent focal length. The image size was 5472 × 3648. The nominal flight height was around 181.4 m, and the ground sample distance was 5 cm with a front and side overlap ratio of 80 and 75%, respectively. Before taking the imagery, we marked ground control points (GCPs) along the banks, wherever access to the area was possible, in order to georeference the digital elevation model (DEM). The GCPs were white crosses (around 1 m size), marked using latex painting and easily visible in the aerial imagery. A total of 44 GCPs were marked along the riverbanks and their coordinates measured using a real-time kinematic (RTK) GPS unit. After the GCPs were marked, the UAVs were launched and pictures taken including the GCPs; a total of 1358 pictures were taken during the surveys. The imagery was analysed and processed using Agisoft PhotoScan software, which compares the imagery and finds homologous points in each picture. The GCPs were split into two groups: the first group with 30 GCPs was used to correct the imagery;

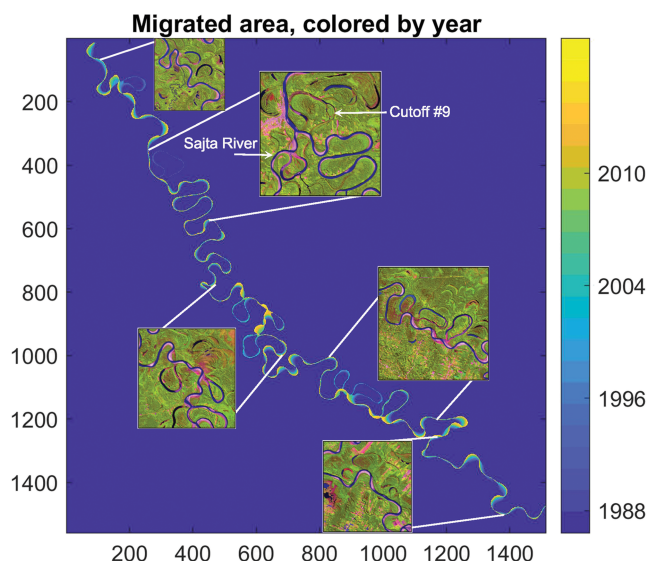


FIGURE 6 Meander migration areas for 30-year period. In zoom, areas where cutoffs were observed [Colour figure can be viewed at wileyonlinelibrary.com]

the second with 14 GCPs was used to assess the accuracy of the imagery. The processed imagery taken in May resulted in orthophotos and a DEM covering around 350 hectares of terrain. The mean positional errors of the 14 reserved GCPs were 0.003, 0.004 and 0.06 m in the x, y and z directions, respectively.

Underwater features of the Ichilo River were measured through bathymetric surveys. An interferometric MBES and an inertial navigation system (INS) was attached to a boat and surveyed along 14 km of the Ichilo River and 2 km of its tributary, the Sajta River. The data can be accessed through the U.S. Geological Survey (USGS) data release website (Kinzel et al., 2019), which includes survey point data (in metres) in Universal Transverse Mercator Zone 20 South. The DEM was created at 1 m resolution and was combined with the DEM obtained from the UAV surveys to obtain cross-sections of the river.

Additionally, soil samples were taken at two point bars in the river, and values for the mean grain size were obtained.

4 | RESULTS

4.1 | Mechanisms of meander migration

Figure 6 serves as evidence of the changing nature of the Ichilo River, showing the paths where the river used to flow through the last 30 years. Moreover, it helps us to identify the location of the migrated areas and the occurrence of cutoffs. As expected in a meandering river, the planform shape indicates that the erosion area was larger in the concave parts of the bends, while the deposition area was observed in their inner part. Furthermore, cutoffs were identified and shown in a detailed zoom (Figure 6). Although we observed both chute cutoffs and neck cutoffs, the dominant type of cutoff in the Ichilo River was the neck cutoff (Figures 6 and 7), with a total of 10 neck cutoffs in our studied area. The largest cutoff in terms of area observed in the Ichilo River corresponds to a human-induced cutoff (cutoff #9, Figures 6 and 7), located near the confluence with the Sajta River.

The annual reach-averaged migration rates of the Ichilo River for the analysed period are presented in Figure 8. The reach considered in the calculations corresponds to the river length shown in Figure 6. An increase in migration rates is observed from 2005, with a peak occurring in 2008. The spike in migration rates measured after 2005 seems to correlate with the occurrence of many cutoffs. Four cutoffs were observed between 2007 and 2010, together with an increase in the annual averaged river width as observed in Figure 8b. Again, after 2014–2015 two cutoffs were observed and also correlate with increases in the annual averaged river width.

From November 2007 to April 2008, Bolivia suffered a severe season of flooding where the city of Puerto Villarreal was affected by La Niña events. The data indicate that the Ichilo River remained flooded for 5 days in January 2008, with water levels over bank level (>7.8 m). Another event of high precipitation was registered in 2014, when water levels remained over bank level for almost 23 days, being the largest event registered in the 30-year period. It is possible that the high meander migration rates in 2008 were related to the high-precipitation event occurring in that year, and this could have triggered the development of the cutoffs that were observed in the following years.

Similar to the event of 2008, the high precipitation observed in 2014 seemed to have promoted the occurrence of cutoffs and increased the river width, but no change in meander migration rates was observed.

Furthermore, the maximum annual stage (S_{max}) was plotted against the annual averaged migration rate (M_{rcd}) (Figure 9a), and the results show a small to moderate correlation ($R^2 = 0.16$).

Two points in the Ichilo River, cutoff #F1 and cutoff #F2 (see location in Figure 7) were identified to be susceptible to the occurrence of a cutoff. We compared the evolution of the distance before cutoff occurrence in both sections using satellite imagery and orthophotos (Figure 9b). The graph indicates that the distance across the neck of #F1 decreased at a faster rate than in #F2. The distance across the neck in #F1 decreased by 87.4% of the initial distance (761.7 m) in 1988, while the neck distance in #F2 decreased 47.8%

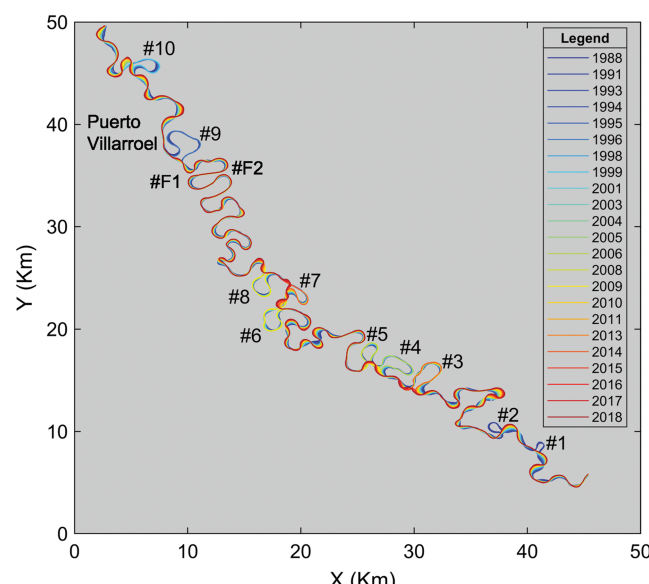


FIGURE 7 Centreline migration and number of cutoffs observed via oxbow lakes in the Ichilo River. #F1 and #F2 show the location of two possible cutoffs expected to occur in the near future [Colour figure can be viewed at wileyonlinelibrary.com]

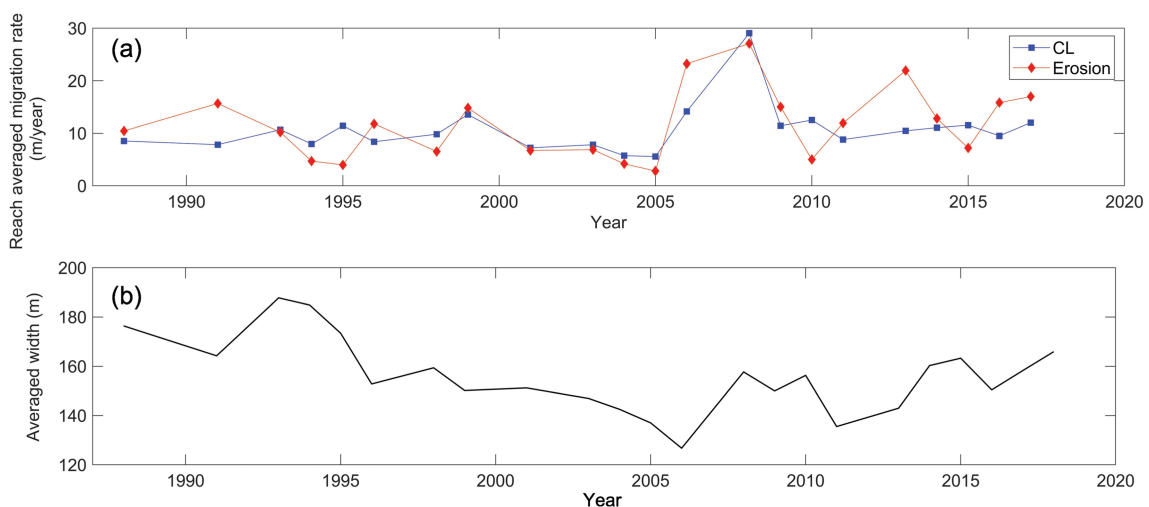


FIGURE 8 (a) Reach-averaged migration rate per year, based on centreline migration (CL), based on erosion (erosion) and (b) annual averaged width variation in the studied period [Colour figure can be viewed at wileyonlinelibrary.com]

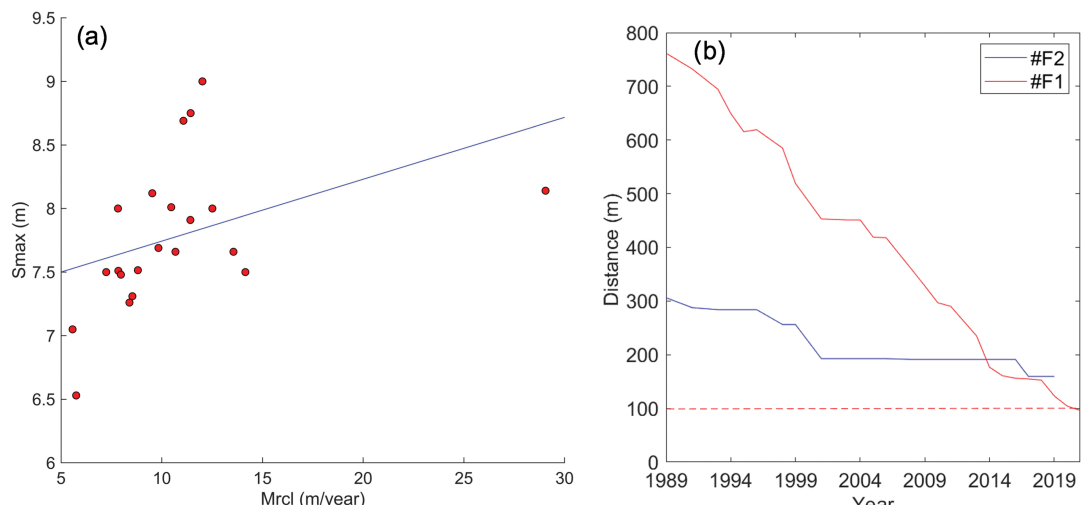


FIGURE 9 (a) Correlation between annual maximum stage and migration rates; (b) evolution of the distance across the neck before the occurrence of a cutoff event for #F1 and #F2 [Colour figure can be viewed at wileyonlinelibrary.com]

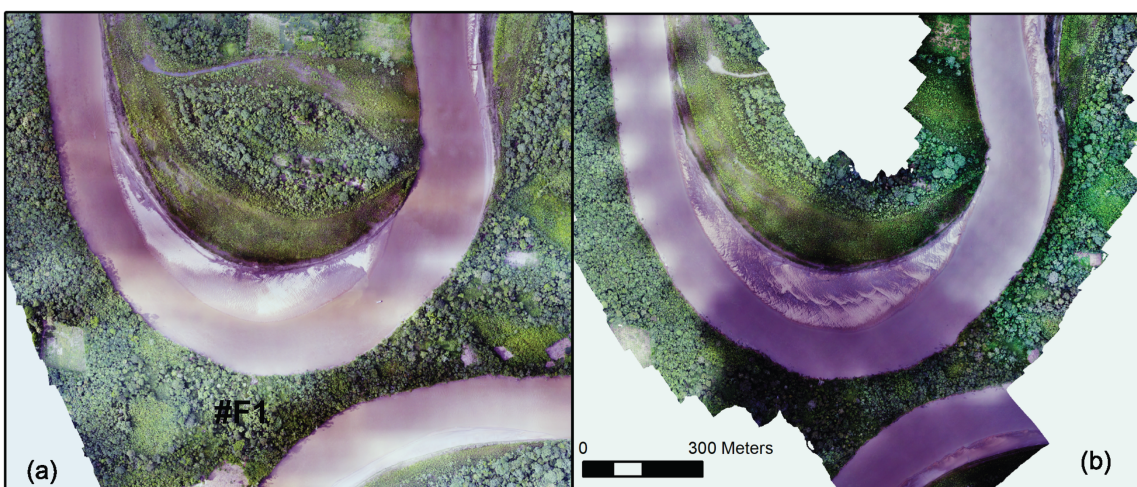


FIGURE 10 Comparison of the orthophotos taken in the area where cutoff #F1 is expected to occur (see location at Figure 7) [Colour figure can be viewed at wileyonlinelibrary.com]

only. Our last field measurement (from the orthophotos obtained in May 2019) showed that the distance left to the intersection and formation of cutoff in #F1 (neck) was 96.1 m. Figure 10 compares the orthophotos in the location of cutoff #F1 for the months of (a) February and (b) May 2019.

4.1.1 | Spatiotemporal distribution of channel widths

Lopez Dubon and Lanzoni (2019) discussed how width fluctuations can be described by a GEV probability distribution. In the case of the Ichilo River we applied many PDFs and found that a GEV distribution is the best fit for the period 1988–2013, while from years 2014 to 2018 an inverse Gaussian distribution represents the variation of the

data better. An example of the analysis of the histograms and the fitted PDFs for years 1988 and 2018 is shown in Figure 11.

The annual PDFs of the Ichilo River in the studied period are presented in Figure 12a. In the period of Figure 12b, three cutoffs were observed in years 2008, 2009 and 2010, and in Figure 12c cutoffs occurred in years 2014 and 2015. The main changes in the PDFs occurred in years with cutoffs, while in years without cutoffs (2016–2018) the PDFs' shape remained similar.

4.1.2 | Bank erosion and bed topography

Bends in the Ichilo River are characterized by stable vertical cutbanks, constituted of a mixture of cohesive material and fine sand. The PET test suggests that the material in the banks is highly erodible in the

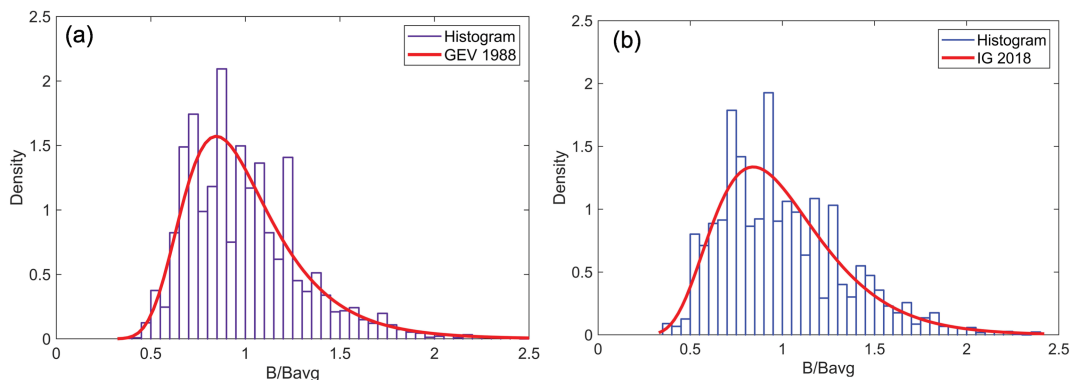


FIGURE 11 Histograms and the best-fit probability distribution function for years (a) 1988 and (b) 2018. GEV = generalized extreme value, IG = inverse Gaussian [Colour figure can be viewed at wileyonlinelibrary.com]

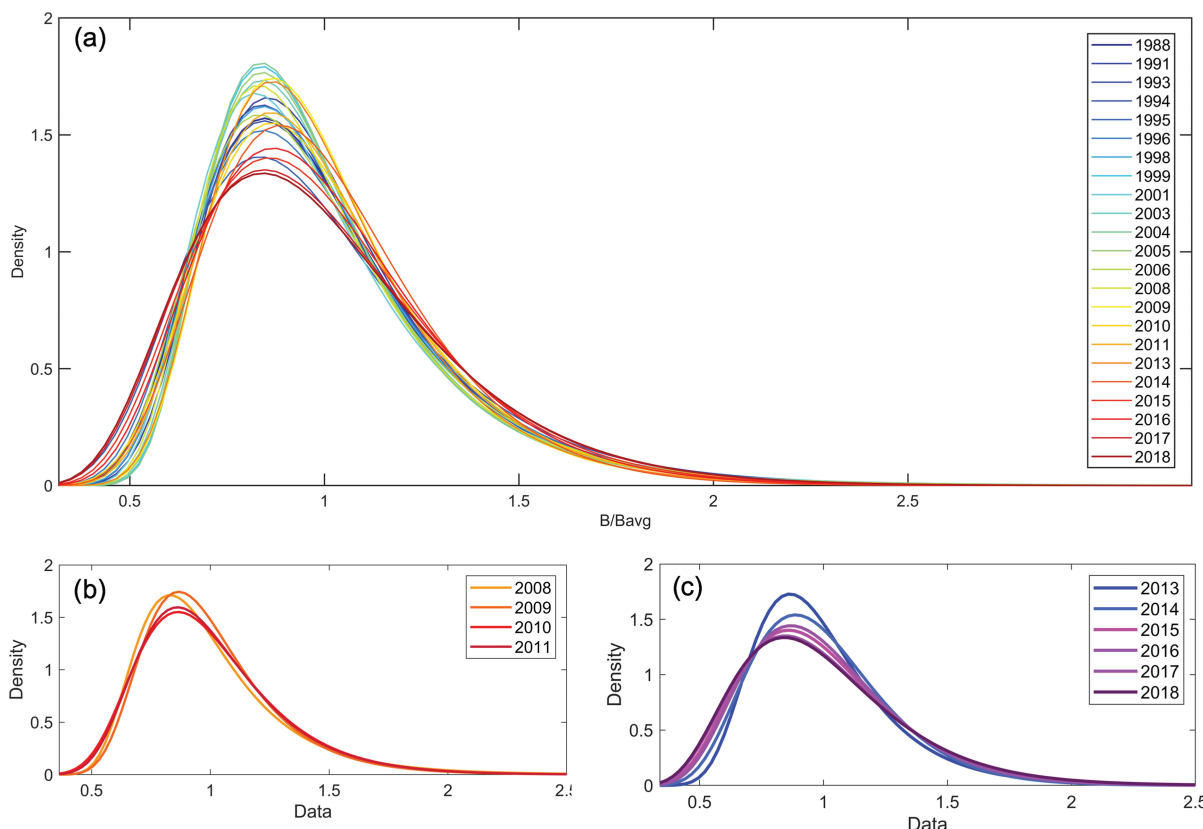


FIGURE 12 (a) Probability distribution functions for all the studied period in the Ichilo River; (b) period 2008–2011; (c) period 2013–2018 [Colour figure can be viewed at wileyonlinelibrary.com]

area near the port (Figure 13b). Upstream the confluence of the Ichilo River with the Sajta River, the floodplain is covered by a dense forest (Figure 13a). The inner part of the bends is mainly constituted of fine sand, where the vegetation is composed of small bushes. The structure of the points bar is presented in Figures 13c and d. Excavations made *in situ* showed two layers of material deposited and clearly separated by a small layer of finer material. Two sediment samples were taken in the Ichilo River with the following mean grain size D_{50} : 0.106 mm (sample 1) and 0.210 mm (sample 2). The location where the samples were taken is presented in Figure 14. Furthermore, Figure 14 shows the measurements of the bed topography with the MBES and the orthophotos collected during the second field survey. Both measurements are in good agreement. In Figure 15, the data from the UAVs and the MBES bathymetry were combined in order to obtain cross-sectional profiles of the banks of the Ichilo River, showing high consistency between the results of the UAVs and the sonar. Some areas could not be surveyed because the boat could not reach these locations due to shallow water and the presence of vegetation that obstructed access. The maximum water depth retrieved during the measurements was around 14 m near the area of the port. Another point of interest was located downstream of the confluence, where the difference in riverbed elevation of the Ichilo and Sajta rivers was around 10 m (Figures 14 and 15, section C-C').

Bank failures were observed all along the Ichilo riverbanks (Figure 15). In general, mass failures are concentrated in areas where the hydrodynamic conditions and topographic and geotechnical properties of the banks induce mass failures (Motta et al., 2014), particularly in the bend apex where outer banks with cohesive materials are steeper and taller, such as in the case of the Ichilo River.

There are different factors that influence the shear stress distribution on banks in meandering bends, such as secondary flow strength, bank slope, width-to-depth ratio, difference in roughness between bed and planform evolution (Motta et al., 2014). Flow in a cross-sectional bend is directed from the inner bank (bar) towards the outer bank (pools) due to the topography of the riverbed. Whenever this effect is strong, the locus of maximum flow velocity occurs

towards the outer bank, leading to bank retreat due to continued action of erosion of the bank. The eroded material, depending on the size and discharge of the river, can remain in front of the bank, as observed in some cross-sections of the Ichilo River. If the deformation is prominent, the locus of maximum flow velocity occurs over the pools close to the banks. Direct action of the flow on the bank in these regions leads to bank retreat through continuous erosion of the bank (Ferreira da Silva & Ebrahimi, 2017). In the Ichilo River, bed erosion in the outer bank downstream of the channel apex of bend #F1 (Figure 14d) indicates a full development of secondary flow.

In addition, changes in the bed profile of the river can be better appreciated in (Figure 15), where two deep holes were observed, one corresponding to the location of the confluence and the other corresponding to the area of the port. The slope of the river calculated from the profile in Figure 15 was $S = 0.00022$.

5 | DISCUSSION

This research highlights the need for field works combined with spatiotemporal satellite imagery analysis to study the planform dynamics of small meandering rivers such as the Ichilo. The results from the satellite imagery allowed us to identify the neck cutoffs as main controls on the planform evolution of the Ichilo River. In addition, the analysis of two bends of the Ichilo River (#F1 and #F2) has shown the spatial variability of the migration rates and the interaction between bends under similar hydraulic conditions. Further changes in the planform shape of these bends of the Ichilo River are likely to happen in the short term. We expect the development of cutoff #F1 for several reasons. First, the distance across the neck in #F1 has been decreasing at a higher rate than in #F2 due to the growth of the point bar, which narrows the channel and increases the velocity of the flow towards the outer bank (bar push theory) (van de Lageweg et al., 2014). The satellite imagery showed that the point bar in #F1 is bigger than the point bar in #F2. In addition, in the case of #F1, the neck is experiencing erosion from both sides due to the skewness of the bend and the

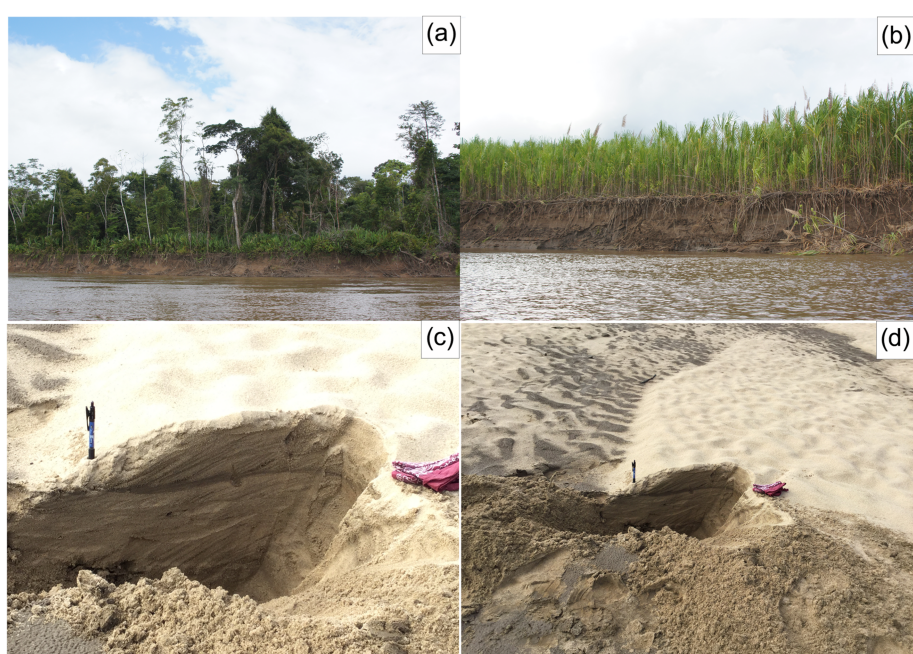


FIGURE 13 Typical banks observed along the Ichilo River: (a) dense forest over cohesive material; (b) banks with small bushes; (c, d) stratigraphy in a point bar of Ichilo River [Colour figure can be viewed at wileyonlinelibrary.com]

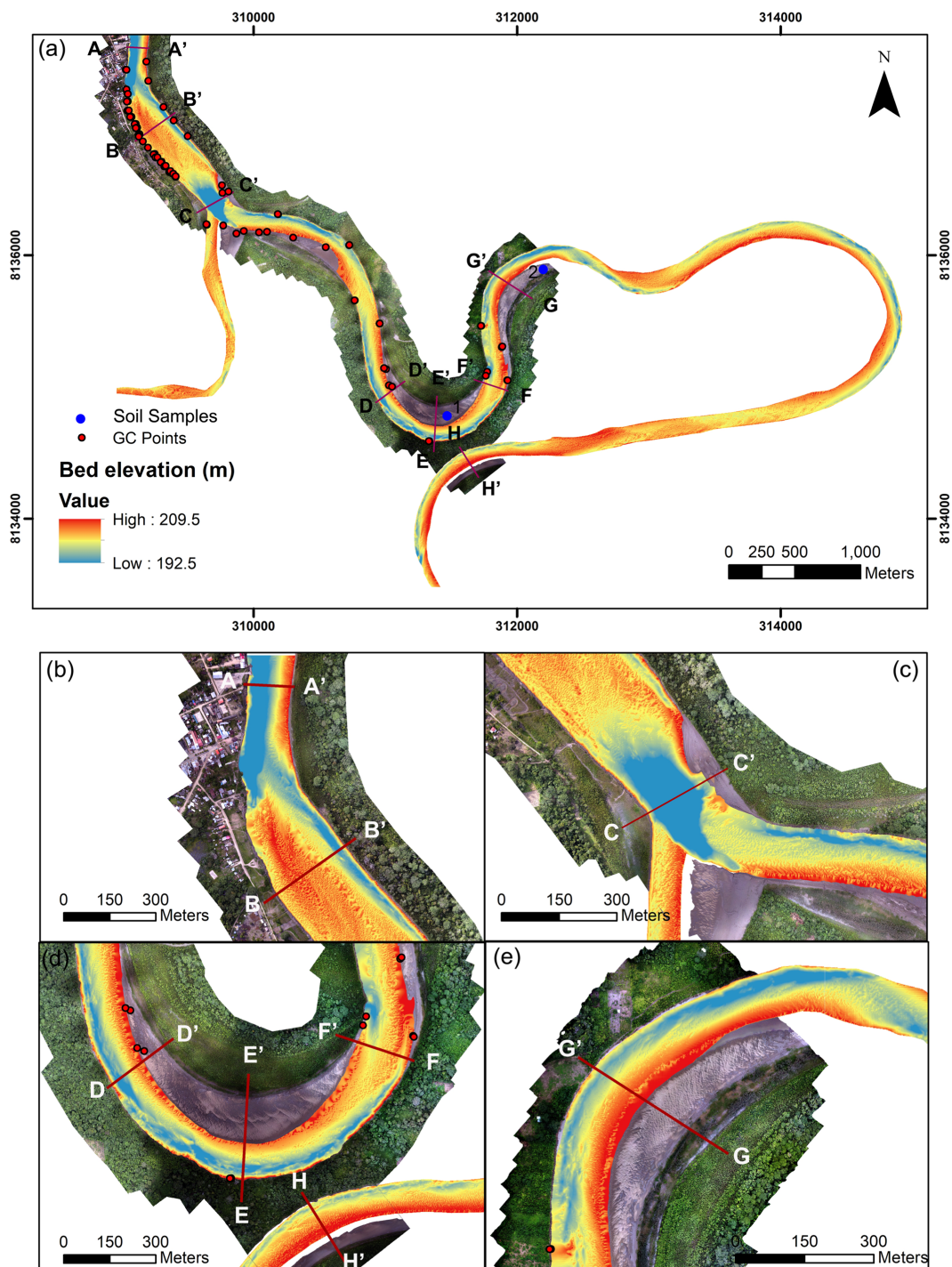


FIGURE 14 Bathymetry obtained with the MBES and orthophotos taken with the UAV in May 2019. (a) Area of study and location of the GCPs and soil samples; (b–e) zoom at different parts of the Ichilo River (see location of the field surveys in Figure 1) [Colour figure can be viewed at wileyonlinelibrary.com]

geometry of the channel, while erosion in #F2 is occurring mainly on one side. The bathymetric data confirm this information, where in the case of #F1 the erosion is observed along both sides of the neck, while in the case of #F2 the erosion concentrates downstream of the neck. As the distance across the neck decreases, intra-meandering flow inside the banks may increase from one bank and that could accelerate the process.

Planform evolution depends on the magnitude and duration of the high and low flow discharges (Asahi et al., 2013). In the Ichilo River, we observed high variability in water levels. It is expected that the river behaves differently during increasing and decreasing of the

discharge, affecting the accretion and erosion processes. High and lower flows seem to govern bank accretion, where vertical accretion occurs during floods and transverse point bar accretion during the falling stage and normal flows (Crosato, 2008). Also, heavy precipitation may trigger mass failures along the banks due to positive pore pressures that reduce the effective friction angle in the banks (Thorne, 1991). During our field works we observed mass failures along the banks which corresponded to a low flow state. In our study, annual migration rates showed a correlation with higher water levels in the river. A similar effect was observed by Schwenk et al. (2017) in his analysis of the Ucayali River and by Gautier et al. (2010) in the

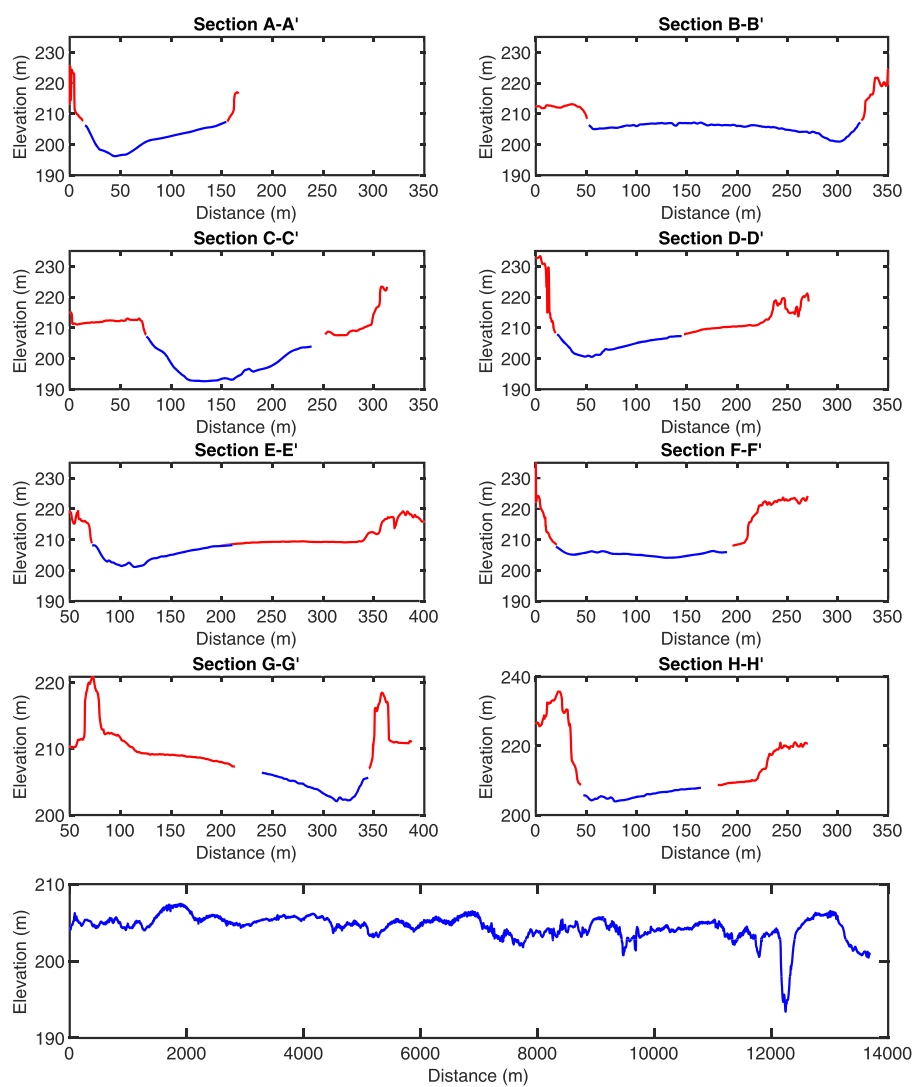


FIGURE 15 River cross-sections and bed elevation profile retrieved at different locations along the Ichilo River. The y-axis shows the elevation and the x-axis shows the distance. Red lines were retrieved with the UAVs and blue lines show the bathymetric data obtained with the MBES [Colour figure can be viewed at wileyonlinelibrary.com]

Beni River. The higher annual migration rates in the year 2008 coincided with La Niña years, which affected Bolivia with extreme precipitation events. The city of Puerto Villarreal suffered inundations from the Ichilo River that lasted 5 days. As inundation periods in the Ichilo River are usually shorter, a large period of inundation may have affected the strength in the banks, triggering bank failures along the river. In addition, another much larger high-precipitation event was observed in 2014, where the river remained inundated for 23 days and, in the following years, two cutoffs were observed. Human-induced cutoffs observed in the Ichilo and Sajta rivers illustrate the impact of human intervention in the planform development of the Ichilo River. The case of cutoff #9, the human-induced cutoff, as a response to a natural neck cutoff that threatened the safety of the port infrastructure, consisted in the design of a new alignment for the Ichilo River and its tributary (Peters, 2009). This design considered a mild curvature at the confluence of the Sajta and Ichilo rivers in order to avoid the generation of secondary flows that would promote bank erosion in Ichilo riverbanks (Peters, 2009) and the cutoff in the Ichilo River. If the natural meander cutoff had developed, the port would have been left in the abandoned path (oxbow lake), eventually becoming useless (Peters, 1998); and the current planform shape of the Ichilo River would have changed to a different configuration.

In addition, areas where the river is stable and has not migrated in the period of our investigation were identified. The inactivity of these

areas may be related to the planform spatial variability due to geological reasons (Peters, 1998). For example, the area between the port and the intersection with the Sajta River has maintained the original planform shape since 1988 with minor modifications, even though the PET showed that the bank material is highly erodible, and according to Peters (1998), this may be the reason why the inhabitants in earlier times decided on that location to establish the port. However, even though only minor planform changes were observed in this area, the high-resolution bathymetric data showed scour holes in the bed topography in the area near the port and near the confluence with the Sajta River. The collapse of the platform of the port at the location of the scour hole, in September 2019, showed that the bed topography is also changing. The confluence with the Sajta River affects the riverbed morphology, as shown by the formation of the scour hole downstream of the confluence and deposition of this material downstream in section B-B' (Figure 14b).

In addition, the growth of the city along the Ichilo riverbanks has brought modification to the natural state of the river. In order to protect the city against bank erosion, some protection works have been implemented on the banks. These works may have constrained the position and direction of the channel axis in the right bank of the Ichilo River. Furthermore, the location of the protection works coincides with the area where riverbed erosion is observed, as illustrated in Figures 14 and 15. In the absence of this constraint, the meander

would probably evolve continuously until the occurrence of a new cutoff (Lanzoni & Seminara, 2006).

6 | CONCLUSIONS

We studied the planform morphodynamics and riverbed topography of a small meandering river (Ichilo) in the upper part of the Bolivian Amazon basin. Through spatiotemporal remote sensing analysis and field works, we aimed to understand the factors that control the planform evolution of the Ichilo River. Our results showed cutoffs as the main mechanism of planform change of the Ichilo River, together with human interventions. The maximum annual water level showed a small to moderate correlation with the meander migration rates. Also, heavy rainfalls observed in the Ichilo River seem to correlate with the occurrence of cutoffs, increases in the river width and meander migration rates. A spatiotemporal analysis of the width variation has shown that a PDF distribution can describe the river width variation in the Ichilo River. A GEV probability distribution provided the best fit of data for the period from 1988 to 2013, while for the period from 2014 to 2018 an inverse Gaussian distribution showed a better fit. The PDFs presented a similar shape in years with no cutoff, but years with cutoff showed changes in the PDFs. This study highlights the potential of SfM analysis combined with MBES bathymetric surveys to obtain data in areas of remote access, showing us the riverbed and bank changes in great detail. In addition to the aforementioned factors, we want to mention the possibility that the increased rate of forest loss in the last 30 years in the south and southwest area of the Ichilo and Sajta rivers has affected the meander migration rates in the last years of the studied period (post-2005). The spatial variability of meander migration rates was discussed by identifying two points susceptible to cutoffs near the city of Puerto Villaruel. We expect that cutoff #F1 may have developed first. Future cutoff development will present further modifications to the ever-changing landscape of the Ichilo River floodplains. A new cutoff would imply morphological adjustments such as changes in the riverbed topography due to the sudden reduction of the river length. A redistribution of sediments after the event is expected, with an increase in migration rates downstream.

The collapse of the platform of the port located in Puerto Villaruel showed the need for bathymetric data and monitoring of the river. The lack of data on small rivers located in the upper Amazon basin, such as the Ichilo, calls for more field studies in order to guarantee the safety of the riverine communities that rely on them.

ACKNOWLEDGEMENTS

The authors would like to express their thanks to the Ministry of Education, Culture, Sports, Science and Technology (MEXT) of Japan for support to make this work possible; the Nitobe School Project Grant supported by Hokkaido University Frontier Foundation for providing economic support; the Laboratory of Hydraulics of the Mayor of San Simon University (LHUMSS), Servicio de Mejoramiento de la Navegación Amazónica (SEMENA) and Servicio Departamental de Cuenca (SDC) in Bolivia for their collaboration. Comments by Alexander Bryk greatly helped to improve this paper.

Any use of trade, firm, or product names is for descriptive purposes only and does not imply endorsement by the U.S. Government.

CONFLICT OF INTEREST

There is no conflict of interest in this paper.

DATA AVAILABILITY STATEMENT

The dataset of the bathymetric survey and structure from motion of the Ichilo River is openly available [USGS data release] at <http://doi.org/10.5066/P9FW6E8K> and [Dryad] <https://doi.org/10.5061/dryad.jh9w0vt9t>, respectively.

ORCID

Kattia Rubi Arnez Ferrel  <https://orcid.org/0000-0003-1670-3272>
 Jonathan Mark Nelson  <https://orcid.org/0000-0002-7632-8526>
 Yasuyuki Shimizu  <https://orcid.org/0000-0002-1870-5741>
 Tomoko Kyuka  <https://orcid.org/0000-0001-5490-8469>

REFERENCES

- Asahi, K., Shimizu, Y., Nelson, J. & Parker, G. (2013) Numerical simulation of river meandering with self-evolving banks. *Journal of Geophysical Research - Earth Surface*, 118(4), 2208–2229. <https://doi.org/10.1029/jgrf.20150>
- Briaud, J.-L., Bernhardt, M. & Leclair, M. (2012) The pocket erodometer test: Development and preliminary results. *Geotechnical Testing Journal*, 35, 342–352.
- Camporeale, C., Perucca, E. & Ridolfi, L. (2008) Significance of cutoff in meandering river dynamics. *Journal of Geophysical Research - Earth Surface*, 113(F1), 1–11. <https://doi.org/10.1029/2006JF000694>
- Crosato, A. (2008) *Analysis and modelling of river meandering Analyse en modellering van meanderende rivieren*. Amsterdam: IOS Press.
- Ferreira da Silva, A.M. & Ebrahimi, M. (2017) Meandering morphodynamics: Insights from laboratory and numerical experiments and beyond. *Journal of Hydraulic Engineering*, 143(9), 03117005. [https://doi.org/10.1061/\(ASCE\)HY.1943-7900.0001324](https://doi.org/10.1061/(ASCE)HY.1943-7900.0001324)
- Gautier, E., Brunstein, D., Vauchel, P., Jouanneau, J.M., Roulet, M., Garcia, C. et al. (2010) Channel and floodplain sediment dynamics in a reach of the tropical meandering Rio Beni (Bolivian Amazonia). *Earth Surface Processes and Landforms*, 35(15), 1838–1853. <https://doi.org/10.1002/esp.2065>
- Gomes, C.H., Sperandio, D.G. & Dessart, R.L. (2018) Remote sensing analysis of the meanders migration in the Mamorecillo River between 1985 and 2012, Bolivia. *International Journal of Advanced Research in Science*, 5(4), 221–228. <https://doi.org/10.22161/ijaers.5.4.32>
- Gorelick, N., Hancher, M., Dixon, M., Ilyushchenko, S., Thau, D. & Moore, R. (2017) *Google Earth Engine: Planetary-scale geospatial analysis for everyone*. Remote Sensing of Environment. *Remote Sens. Environ.*
- James, M.R., Chandler, J.H., Eltner, A., Fraser, C., Miller, P.E., Mills, J.P. et al. (2019) Guidelines on the use of structure-from-motion photogrammetry in geomorphic research. *Earth Surface Processes and Landforms*, 44(10), 2081–2084. <https://doi.org/10.1002/esp.4637>
- [Dataset] Kinzel, P., Nelson, J.M. & Kattia, R.A.F. (2019) *Bathymetric survey of the Ichilo and Sajta Rivers, near Puerto Villaruel, Bolivia, May 23–24, 2019*. U.S. Geological Survey data release. <https://doi.org/10.5066/P9FW6E8K>
- Lanzoni, S. & Seminara, G. (2006) On the nature of meander instability. *Journal of Geophysical Research - Earth Surface*, 111(F4), 1–14. <https://doi.org/10.1029/2005JF000416>
- Li, J., Grenfell, M.C., Wei, H., Tooth, S. & Ngiem, S. (2020) Chute cutoff-driven abandonment and sedimentation of meander bends along a fine-grained, non-vegetated, ephemeral river on the Bolivian Altiplano. *Geomorphology*, 350, 106917. <https://doi.org/10.1016/j.geomorph.2019.106917>
- Lombardo, U. (2016) Alluvial plain dynamics in the southern Amazonian foreland basin. *Earth System Dynamics*, 7(2), 453–467. <https://doi.org/10.5194/esd-7-453-2016>

- Lopez Dubon, S. & Lanzoni, S. (2019) Meandering evolution and width variations: A physics-statistics-based modeling approach. *Water Resources Research*, 55(1), 76–94. <https://doi.org/10.1029/2018WR023639>
- Motta, D., Langendoen, E.J., Abad, J.D. & García, M.H. (2014) Modification of meander migration by bank failures. *Journal of Geophysical Research - Earth Surface*, 119(5), 1026–1042. <https://doi.org/10.1002/2013JF002952>
- Peters, J.J. (1998) Amélioration du transport fluvial en Amazonie bolivienne. *Bulletin of the International Association for Landscape Ecology - Japan*, 44, 463–482.
- Peters, J.J. (2009) [PRESENTATION] Ichilo-Mamore river (Bolivian Amazon region): Saving the accessibility of a main river harbour threatened by a natural meander cut-off, using original river works and structures. MaRIMorph: Brussels; 34 slides.
- Rejas, D. (2018) Trophic structure of a floodplain fish assemblage in the upper Amazon basin, Bolivia. *Revista de Biología Tropical*, 66(3), 1258–1271. <https://doi.org/10.15517/rbt.v66i3.30693>
- Schwenk, J. & Foufoula-Georgiou, E. (2016) Meander cutoffs nonlocally accelerate upstream and downstream migration and channel widening. *Geophysical Research Letters*, 43(24), 12,437–12,445. <https://doi.org/10.1002/2016GL071670>
- Schwenk, J., Khandelwal, A., Fratkin, M., Kumar, V. & Foufoula-Georgiou, E. (2017) High spatiotemporal resolution of river planform dynamics from landsat: The RivMAP toolbox and results from the Ucayali river. *Environmental Earth Sciences*, 4(2), 46–75. <https://doi.org/10.1002/2016EA000196>
- Schwenk, J., Lanzoni, S. & Foufoula-Georgiou, E. (2015) The life of a meander bend: Connecting shape and dynamics via analysis of a numerical model. *Journal of Geophysical Research - Earth Surface*, 120(4), 690–710. <https://doi.org/10.1002/2014JF003252>
- Thorne, C. (1991) Bank erosion and meander migration of the Red and Mississippi Rivers, USA. *Hydrol. water Manag. large river basins* 20th Gen. Assem. Int. union Geod. Geophys. Vienna. Int. Assoc. Hydrol. Sci. 201, 301–313.
- van de Lageweg, W.I., van Dijk, W.M., Baar, A.W., Rutten, J. & Kleinhans, M.G. (2014) Bank pull or bar push: What drives scroll-bar formation in meandering rivers? *Geology*, 42(4), 319–322. <https://doi.org/10.1130/G35192.1>
- van Dijk, W. (2013) Meandering rivers – feedbacks between channel dynamics, floodplain and vegetation. Utrecht University.

How to cite this article: Arnez Ferrel KR, Nelson JM, Shimizu Y, Kyuka T. Past, present and future of a meandering river in the Bolivian Amazon basin. *Earth Surf. Process. Landforms*. 2021;46:715–727. <https://doi.org/10.1002/esp.5058>